# Bethe-Salpeter Equation at the Critical End Point of the Mott Transition

Erik G. C. P. van Loon,[1,2,*] Friedrich Krien,[3] and Andrey A. Katanin[4,5]
[1]Institut für Theoretische Physik, Universität Bremen, Otto-Hahn-Allee 1, 28359 Bremen, Germany
[2]Bremen Center for Computational Materials Science, Universität Bremen, Am Fallturm 1a, 28359 Bremen, Germany
[3]Jožef Stefan Institute, Jamova 39, SI-1000, Ljubljana, Slovenia
[4]Moscow Institute of Physics and Technology, 141701 Dolgoprudny, Russia
[5]M. N. Mikheev Institute of Metal Physics, Russian Academy of Sciences, 620108 Yekaterinburg, Russia

(Received 27 March 2020; revised 17 August 2020; accepted 21 August 2020; published 23 September 2020)

Strong repulsive interactions between electrons can lead to a Mott metal-insulator transition. The dynamical mean-field theory (DMFT) explains the critical end point and the hysteresis region usually in terms of single-particle concepts, such as the spectral function and the quasiparticle weight. In this Letter, we reconsider the critical end point of the metal-insulator transition on the DMFT's two-particle level. We show that the relevant eigenvalue and eigenvector of the nonlocal Bethe-Salpeter kernel in the charge channel provide a unified picture of the hysteresis region and of the critical end point of the Mott transition. In particular, they simultaneously explain the thermodynamics of the hysteresis region and the iterative stability of the DMFT equations. This analysis paves the way for a deeper understanding of phase transitions in correlated materials.

DOI: 10.1103/PhysRevLett.125.136402

The interplay of interactions, correlations, and quantum statistics in quantum many-body physics is responsible for the appearance of complicated new phases, with the Mott transition [1] as a prominent example. The simplest theoretical realization of this correlation-driven metal-insulator transition (MIT) occurs in the (single-band) Hubbard model [2–5]. Quantum simulators using ultracold fermions in optical lattices are providing unprecedented experimental insight into this transition [6–10].

From the theory side, the dynamical mean-field theory [11,12] (DMFT) provides a rare example of an exact solution to a strongly correlated problem, namely, to the Hubbard model in the limit of infinite dimensions. During the first decade after the DMFT's invention, the essence [13] of the Mott transition was ascertained [16–23]: At the zero temperature transition to the insulating phase, the quasiparticle weight vanishes and the self-energy is divergent at small frequency, in contrast to the Fermi liquid. The $U$-$T$ (interaction-temperature) DMFT phase diagram of the particle-hole symmetric model can be summarized as follows (sketched in Fig. 1; for an overview see Refs. [23–26]): at low temperature, there is a metallic phase at small $U < U_{c1}$ and an insulating phase at large $U > U_{c2}$. In between, for $U_{c1} < U < U_{c2}$, both metallic and insulating solutions can be stabilized. This hysteresis region (shaded blue area) ends at a critical temperature $T_c$, where $U_{c1} = U_{c2} = U_c$ (purple dot). No phase separation occurs in the particle-hole symmetric system [24].

Although the single-particle properties (Green's function, self-energy, quasiparticle weight) are sufficient to understand the essentials of the metal-insulator transition, two-particle properties provide another rich layer of information about the response to external fields, spatial correlations, and optical properties. The simplifications of infinite dimensions allowed early studies at the two-particle level [19,20,27–30], but a systematic investigation of the DMFT two-particle physics had to wait [31–38] for computational improvement, especially the invention of continuous-time quantum Monte Carlo solvers [39–41].

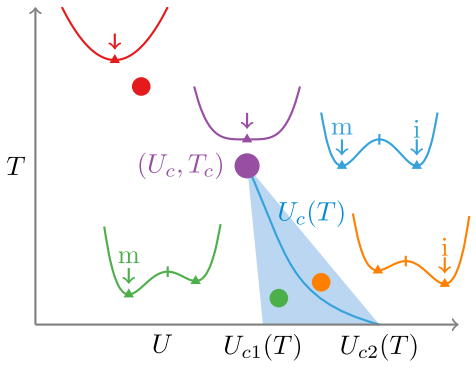


FIG. 1. Sketch of the phase diagram of the particle-hole symmetric Hubbard model in DMFT. The first-order metal-insulator transition occurs at $U_c(T)$ (blue curve), with a second-order critical end point at $(U_c, T_c)$ (purple dot). The shaded area is the hysteresis region, where both metal ($m$) and insulator ($i$) can be stabilized. The colored curves illustrate the free energy landscape at selected points (dots) in the phase diagram, the vertical marks denote the local maxima of the free energy, the triangles indicate the local minima, and the arrows show the global minimum.

 

There has recently been a flurry of activity on divergences on the two-particle level [38,42–46], from simple toy models [47,48] and the Hubbard atom [49] to cluster approaches [50], relating these divergences to unphysical solutions [43,45,51] and to the suppression of fluctuations [52,53]. Crucially, divergences of the irreducible vertex already appear in impurity models and therefore cannot originate in the Mott transition: there is no Mott transition in an impurity model with fixed bath—just as the Brillouin function in Curie-Weiss mean-field theory of the Ising model is smooth—and only the self-consistent adjustment of the DMFT auxiliary impurity provides the opportunity for a phase transition. Thus, on the two-particle level, we also expect the Mott transition to appear via self-consistent feedback, that is, outside the impurity model.

The divergences of the irreducible vertex imply that the eigenvalues of the local charge vertex function and local generalized susceptibility can change sign [38,45,53] and, as a matter of fact, the same holds for the corresponding lattice quantities. This undercuts the original idea of using them for constructing the Landau functional near the Mott transition [54,55] because the curvature of the free energy is supposed to be positive definite for stationary solutions. Indeed, Ref. [55] pointed out that the stationary point of the self-energy functional is not necessarily an extremum. Recently, it was shown [37] that the *nonlocal* Bethe-Salpeter kernel, instead of the full one, is a more appropriate quantity to describe the Mott transition, since it yields positive eigenvalues that approach unity from below. The corresponding symmetric Landau parameter is indeed not affected by the divergences of the irreducible vertex [37,38].

We show here that the nonlocal Bethe-Salpeter kernel, associated with the charge sector, provides an intriguing new view on the Mott transition across the hysteresis region and especially at the critical end point. In particular, it appears in the expression for the second derivative of an appropriate Landau functional for the Mott transition, yielding a positive curvature for stationary solutions, whereas the functionals of Refs. [54,55] should be used at weak coupling. Furthermore, this kernel is directly related to the Jacobian of the DMFT fixed point function 23,25,56]], which determines the stability of iterative solutions. The leading eigenvalue of the kernel is unity at the finite temperature critical end point, signaling the onset of the hysteresis region. Nevertheless, at particle-hole symmetry the frequency structure of the corresponding eigenvector ensures that the compressibility does not diverge (cf. Ref. [57]). Therefore, the nonlocal Bethe-Salpeter kernel determines two apparently separate stability criteria, the thermodynamic and the iterative stability, and the eigenvector frequency structure—given by the difference between insulating and metallic solution—distinguishes between diverging response and exact cancellation.

We consider the Hubbard model describing the competition between localization due to the Coulomb interaction $U$ and delocalization due to the dispersion $t_{\mathbf{k}}$. We use $i$ to label the sites on the periodic lattice and $\mathbf{k}$ to label the corresponding momentum. The model is given by the Hamiltonian

$$H = -\sum_{\mathbf{k},\sigma} t_{\mathbf{k}} c^{\dagger}_{\mathbf{k}\sigma} c_{\mathbf{k}\sigma} + U \sum_{i} n_{i\uparrow} n_{i\downarrow}, \tag{1}$$

where $c^{\dagger}_{\mathbf{k}\sigma}$ is the creation operator for a fermion with momentum $\mathbf{k}$ and spin $\sigma = \uparrow, \downarrow$, and $n_{i\sigma} = c^{\dagger}_{i\sigma} c_{i\sigma}$ is the number operator of electrons with spin $\sigma$ on site $i$. We consider this model in the grand-canonical ensemble at temperature $T$ and chemical potential $\mu$. A central object of interest is the (one-particle) Green's function $G_{\mathbf{k},\nu,\sigma} = -\langle c_\sigma c^{\dagger}_\sigma \rangle_{\mathbf{k},\nu}$ in the Matsubara formalism, where $\nu_n = \pi T(2n+1)$, with $n \in \mathbb{Z}$ as the fermionic Matsubara frequencies. We consider the paramagnetic state and for compactness drop the spin labels.

The DMFT [11,12] provides an approximate solution to this model by setting $\Sigma_{\mathbf{k},\nu} = \Sigma^{\mathrm{AIM}}_{\nu}$, where AIM stands for an auxiliary impurity model consisting of a single interacting site in a self-consistently determined bath. For the present discussion, it is sufficient to state that the auxiliary impurity model serves as a tool to evaluate the functional relation $\Sigma[\Delta]$ between the bath hybridization function $\Delta$ and the self-energy $\Sigma$ of the AIM (in practice, we use the ALPS [58] and iQIST [59,60] realizations of CTQMC [41] solver of Ref. [61] with improved estimators [62]). The hybridization $\Delta$ of the auxiliary impurity model is chosen so that the mean-field self-consistency equation $g_\nu[\Delta] = f(\Delta_\nu, g_\nu[\Delta])$ is satisfied. Here $g_\nu[\Delta] = 1/(i\nu_n - \Delta_\nu - \Sigma_\nu)$ and

$$f(\Delta_\nu, g_\nu) = \sum_{\mathbf{k}} G_{\mathbf{k},\nu} = \sum_{\mathbf{k}} \frac{1}{g_\nu^{-1} + \Delta_\nu + t_{\mathbf{k}}}; \tag{2}$$

from now on $\sum_{\mathbf{k}} \equiv (1/N) \sum_{\mathbf{k}\in \mathrm{BZ}}$ denotes the momentum average over the Brillouin zone. The square brackets denote functional relations.

In this Letter, we consider the two-dimensional square lattice Hubbard model, $t_{\mathbf{k}} = 2t(\cos k_x + \cos k_y)$ at half filling. The energy scale is set by $4t = 1$. The half filled model is particle-hole symmetric, which leads to $\mathrm{Re} g_\nu = 0$ and $\mathrm{Re}\Sigma_\nu = U/2$. In other words, only the imaginary parts of both quantities are of interest, which simplifies the analysis.

*Fixed point equation.*—The auxiliary impurity model is a finite system that cannot undergo a (finite temperature) phase transition by itself. Instead, as in Weiss's mean-field theory of magnetism, it is the self-consistency condition that opens the possibility of a phase transition. Therefore, our analysis of the critical point starts with the self-consistency condition.

DMFT looks for solutions of Eq. (2), i.e., a fixed point $\Delta^* = h[\Delta^*]$, where $h[\Delta] = i\nu_n - \Sigma_\nu[\Delta] - 1/f(\Delta_\nu, g_\nu[\Delta])$. To avoid issues related to the noninvertibility [43] of the mapping $\Delta \mapsto g$, we perform the stability analysis in terms of the iterative scheme $\Delta^{(n+1)} = h[\Delta^{(n)}]$. An important question is if these iterations converge to the fixed point $\Delta^*$ if one starts the iteration close to $\Delta^*$. In that case, the fixed point is called attractive [63]. The textbook analysis, based on a linear expansion of $h$ around the fixed point, shows that $\Delta^*$ is attractive if and only if all eigenvalues of the Jacobian $\mathcal{J}|_{\Delta^*} = (\delta h/\delta\Delta)|_{\Delta^*}$ have magnitude smaller than 1. Any eigenvalue larger than 1 implies that the self-consistency cycle is repulsive along the direction given by the corresponding eigenvector. For DMFT, the Jacobian can be evaluated explicitly in Matsubara space as (see Supplemental Material [64])

$$\hat{\mathcal{J}}_{\nu\nu'} = \hat{x}^{-1}\hat{\mathcal{D}}_{\nu\nu'}\hat{x}, \tag{3}$$

$$\mathcal{D}_{\nu\nu'} = T\left(\sum_{\mathbf{k}} G^2_{\mathbf{k},\nu} - g^2_\nu\right) F^{\mathrm{loc}}_{\omega=0,\nu\nu'}, \tag{4}$$

where $F^{\mathrm{loc}}_{\omega,\nu\nu'}$ is the full local charge vertex, and $\hat{x}_{\nu\nu'} = -T\delta_{\nu\nu'} g_\nu g_{\nu'}$ is the local "bubble". The hat denotes a matrix in Matsubara space and, when possible, the matrix indices $\nu$ and $\nu'$ are dropped. The essential element of Eq. (3) is the nonlocal Bethe-Salpeter kernel $\mathcal{D}$ at $\mathbf{q} = 0$ and $\omega = 0$, a quantity that also appears in the calculation of linear response functions based on a decomposition into local and nonlocal fluctuations.

*Response functions.*—Indeed, the DMFT recipe provided above not only allows us to determine the one-particle Green's function $G$ for a given set of parameters $(U, \mu, T)$, but on top of this, DMFT also describes how the system would (linearly) respond [12] to an external field with frequency $\omega$ and momentum $\mathbf{q}$. We restrict our analysis to time-independent fields, $\omega = 0$. The response function $\chi_{\mathbf{q}=0}$ can be obtained from

$$\hat{\chi}^{\mathrm{DMFT}}_{\mathbf{q}=0} = (\hat{1} - \hat{x}\,\hat{F})\frac{\hat{1}}{\hat{1} - \hat{\mathcal{D}}}\hat{X}_{\mathbf{q}=0}, \tag{5}$$

where $(\hat{X}_{\mathbf{q}})_{\nu\nu'} = -T\delta_{\nu\nu'}\sum_{\mathbf{k}} G_{\mathbf{k},\nu}G_{\mathbf{k}+\mathbf{q},\nu}$ is the full bubble, and the fraction denotes matrix inversion in Matsubara space. The relation (5), which is derived in the Supplemental Material [64], is a resummation [31,65–67] of the more familiar expression [12] $\hat{\chi} = (1 + \hat{X}\hat{\Gamma})^{-1}\hat{X}$ that avoids the divergences of the irreducible vertex $\Gamma$. From this generalized susceptibility matrix, the physical response function is obtained as a sum over both fermionic frequencies. For example, the compressibility $dn/d\mu$ is obtained from the generalized susceptibility at $\mathbf{q} = 0$ (and, as before, $\omega = 0$),

$$\frac{dn}{d\mu} = \sum_{\nu\nu'} (\hat{\chi}^{\mathrm{DMFT}}_{\mathbf{q}=0})_{\nu\nu'}. \tag{6}$$

The response in DMFT is thermodynamically consistent in the sense that this Bethe-Salpeter determination of $dn/d\mu$ gives the same result as changing $\mu$ explicitly and calculating the change in $n$ [68].

*Landau theory.*—Following Landau, the free energy functional is the essential ingredient for understanding stable and unstable phases and hysteresis close to the critical point. Characteristic free energy curves are sketched in Fig. 1. The second derivative of the free energy determines if the stationary point is a local minimum ($\delta^2 F > 0$, stable, denoted by triangles in Fig. 1) or a local maximum ($\delta^2 F < 0$, unstable, denoted by a vertical bar). The critical point is where a stable point turns unstable; in other words, $\delta^2 F = 0$ exactly at the critical point (purple curve in Fig. 1).

The Mott transition on the Bethe lattice has been studied using Landau theory [23,69,70]. Here we generalize this approach to arbitrary dispersion $t_{\mathbf{k}}$. With the hybridization $\Delta$ as the order parameter, we write the Landau functional $\Omega$ as $\Omega[\Delta] = \Omega_{\mathrm{imp}}[\Delta] - \Omega'[\Delta]$ (see Supplemental Material for more details [64]), where $\Omega_{\mathrm{imp}}$ is the thermodynamic potential of the auxiliary impurity model. $\Omega'$ provides the nonlocal feedback and ensures that the first derivative $\delta\Omega/\delta\Delta = 0$ at the self-consistent DMFT solution, that is,

$$\frac{\delta\Omega}{\delta\Delta_\nu} = T(g_\nu[\Delta] - g^{\mathrm{sc}}_\nu[\Delta]), \tag{7}$$

where $g_\nu[\Delta] = \delta\Omega_{\mathrm{imp}}[\Delta]/\delta\Delta_\nu$, is the local Green's function determined from the AIM for a given hybridization $\Delta$, and $g^{\mathrm{sc}}[\Delta] = \delta\Omega'/\delta\Delta$ is the solution of the self-consistency condition $g^{\mathrm{sc}}_\nu = f(\Delta_\nu, g^{\mathrm{sc}}_\nu[\Delta])$ for a given $\Delta$, see Eq. (2). We note that the map $\Delta \mapsto g^{\mathrm{sc}}$ can be multivalued. However, as we argue in the Supplemental Material [64], at sufficiently strong coupling (e.g., near the MIT), only one branch is relevant.

To determine the stability of this solution, we proceed with the second derivative (Hessian), which reads (see Supplemental Material [64])

$$\frac{\delta^2\Omega}{\delta\Delta_\nu\delta\Delta_{\nu'}} = -\frac{\hat{1}}{\hat{1} - \hat{x}^{-1}\hat{X}}(\hat{1} - \hat{\mathcal{D}})\hat{x}. \tag{8}$$

This is a matrix equation in Matsubara space, and $\delta^2\Omega/\delta(i\Delta)^2$ is the Hessian matrix, which is a real matrix in the case of particle-hole symmetry. The factor $(\hat{1} - \hat{x}^{-1}\hat{X})^{-1}$ is diagonal in frequency, and, as we discuss in the Supplemental Material [64], in the entire region of interest it has only positive elements; therefore, the stability is determined by eigenvalues of $\hat{1} - \hat{\mathcal{D}}$. At the critical point, the Hessian changes from stable to unstable; i.e., one

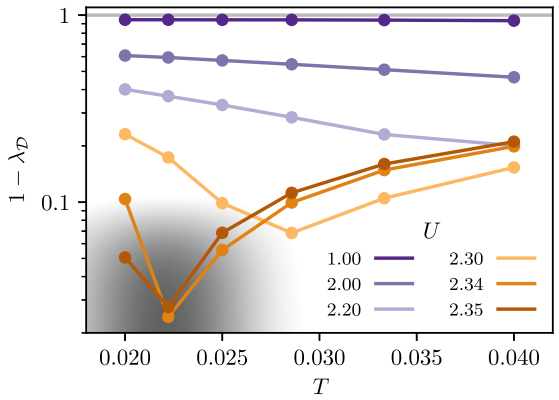


FIG. 2. The leading eigenvalue (note the logarithmic scale) of $\hat{\mathcal{D}}$ approaches unity close to the critical point, $2.3 < U_c < 2.35$ and $0.02 < T_c < 0.025$ (gray region).

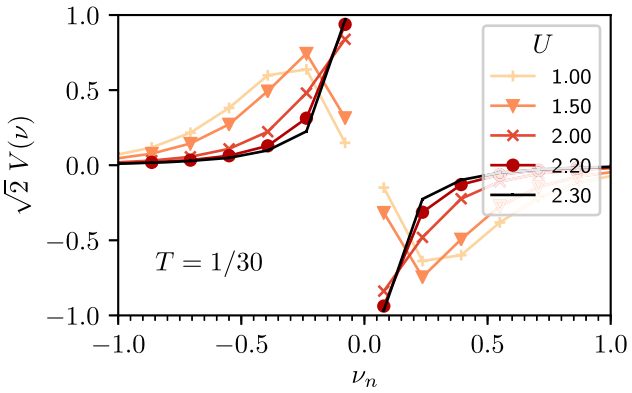


FIG. 3. The leading right eigenvector $V$ of the nonlocal Bethe-Salpeter kernel $\hat{\mathcal{D}}$, for $T$ just above $T_c$. As $U$ increases and the Mott transition is approached, the eigenvector localizes around $\nu = 0$ and $\lambda \to 1$. The eigenvector is normalized to $\sum_\nu |V(\nu)|^2 = 1$.

eigenvalue of $\delta^2\Omega/\delta\Delta^2$ is equal to zero, which requires an eigenvalue of unity for $\hat{\mathcal{D}}$.

The same nonlocal Bethe-Salpeter kernel $\hat{\mathcal{D}}$ has appeared three times in stability criteria: in the Jacobian of the fixed point equation, in the compressibility, and in the second derivative of the self-energy functional. The latter two relate to the *stability* of the physical solution, whereas the Jacobian determines the *attractiveness* of the fixed point in an iterative scheme. For DMFT, these two aspects are tied together by a single kernel.

This allows us to create a unified picture of the hysteresis region of the particle-hole symmetric metal-insulator transition. At the critical end point $(U_c, T_c)$, the purple dot in Fig. 1, the two stable (triangles in Fig. 1) and the one unstable (vertical marks in Fig. 1) stationary points merge together. Therefore, the quadratic part of the free energy functional vanishes at this point (purple curve), which together with Eq. (8) means that the Bethe-Salpeter kernel $\mathcal{D}$ has an eigenvector $V$ with eigenvalue $\lambda \to 1$ (Fig. 2) exactly at the critical end point. Since $\hat{\mathcal{D}}$ is related to the Jacobian of the fixed point equation, the stable and unstable solutions correspond to attractive and repulsive fixed points, respectively [25].

Figure 3 shows the leading right eigenvector $V$ of $\hat{\mathcal{D}}$ close to the critical end point. The physical meaning of this eigenvector is that it relates the three fixed points that exist at $T < T_c$, as $\Delta_m(\nu) - \Delta_u(\nu) \propto (T_c - T)^\beta V(\nu)$ and $\Delta_i(\nu) - \Delta_u(\nu) \propto (T_c - T)^\beta V(\nu)$, where $\Delta_m$, $\Delta_i$, and $\Delta_u$ are the hybridization functions at the metallic, insulating, and unstable fixed points, respectively, and $\beta$ is a critical exponent. This together with particle-hole symmetry $[\Delta(\nu) = -\Delta(-\nu)]$ implies $V(\nu) = -V(-\nu)$, i.e., the eigenvector $V$ is antisymmetric [53]. As the difference between solutions, $V$ provides the "order parameter"—similar to the $\delta\Delta_L$ at $T = 0$ of Kotliar *et al.* [69]—in the sense of Landau's functional: At the critical point, the free energy landscape goes from a parabola to a double well potential along the direction given by $V$. Figure 4 shows that the second derivative of the grand potential—along the direction given by the right eigenvector $W_R$ of the Jacobian—indeed goes to zero as one gets close to the Mott critical end point. Note that the figure is at $T > T_c$, so the second derivative does not quite reach zero.

Since $V(\nu) \sim \delta_{\nu,\nu_0} - \delta_{\nu,-\nu_0}$ at the critical point (cf. Fig. 3), the three solutions $\Delta(\nu)$ differ only at low frequency, i.e., close to the Fermi level. This is in agreement with what is known qualitatively from investigations of the density of states: the difference between the insulator and the metal is that the latter has a quasiparticle peak at the Fermi level. Astretsov *et al.* [71] used a single Matsubara frequency approximation to study the cuprates; our result here is a direct quantitative proof that this kind of approximation is justified at the critical end point of the Mott transition.

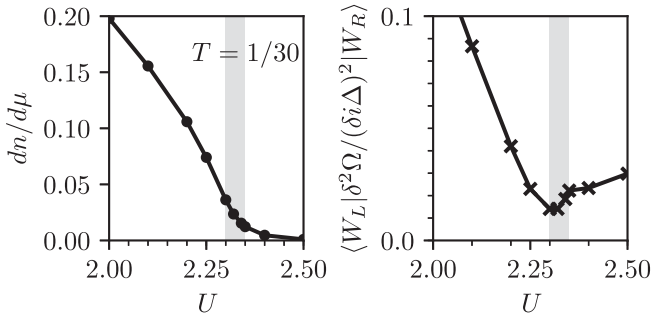


FIG. 4. Left: the compressibility does not diverge as the Mott transition is approached. Right: the second derivative of the Landau functional $\Omega$ determines the thermodynamic stability. Approaching the Mott critical point, the vanishing of this second derivative (in the direction given by $W_R$) signals the onset of the phase transition. Here, $W_{R,L} = g_\nu^{\pm 2}$, where $V$ is the leading right eigenvector of the nonlocal Bethe-Salpeter kernel (cf. Fig. 3), and $T = 1/30 > T_c$. The gray band indicates the vicinity of the Mott transition, $2.3 < U_c < 2.35$.

At $T < T_c$ and $U_{c1} < U < U_{c2}$, the Bethe-Salpeter equation is convergent (and the iterative scheme is attractive) at both the metallic and the insulating solutions $\lambda < 1$ and divergent (repulsive) at the unstable fixed point $\lambda > 1$. Although both metallic and insulating solutions are attractive fixed points, only one of them is the global minimum (c.f., green and orange curves in Fig. 1) of the free energy in most of the hysteresis region. Only at $U_c(T)$ (the blue line in Fig. 1) do both solutions have exactly the same free energy, and this is where the phase transition occurs. At $U_{c1}$ ($U_{c2}$), the unstable and insulating (metallic) fixed point merge, so that $\lambda = 1$ at this fixed point, but the metallic (insulating) solution, with $\lambda < 1$, is the global minimum of the free energy.

Kotliar *et al.* [72] predicted a compressibility divergence at the critical end point of the doping-driven Mott transition, $dn/d\mu \to \infty$. On first sight, our present eigenvalue analysis seems to imply the same, since the Bethe-Salpeter equation (BSE) diverges. However, a divergence in the BSE can be canceled by an exact orthogonality [53,72], and that is indeed what happens at particle-hole symmetry [57]. The eigenvector $V \propto \Delta_m - \Delta_i$ is antisymmetric in $\nu$ and therefore does not contribute to the sum in Eq. (6) [52,53,57], so that $dn/d\mu$, shown in Fig. 4, is finite (and small [73]) at the critical end point. This is consistent with the absence of phase separation at particle-hole symmetry [24]. A nondivergent compressibility combined with a divergence of the BSE is reminiscent of the zero temperature case [37]; in other words, both critical end points of the particle-hole symmetric Mott transition are characterized by a divergent BSE without a divergence in $dn/d\mu$.

The situation away from particle-hole symmetry is more complicated because of the complex valuedness of Green's functions [57]. The antiferromagnetic transition in DMFT [16]—which occurs when the assumption of paramagnetism is lifted—can also be analyzed along the lines of the current Letter as a divergence of the BSE in the magnetic channel. An important open question is the generalization of our analysis to the instabilities found in multiorbital Hund's physics [74–81] and, more generally, to systems that show phase separation [24,72,82–90].

In conclusion, we identified the nonlocal Bethe-Salpeter kernel with the Jacobian of the DMFT fixed point equation and with the curvature of the free energy functional. Near the critical end point of the finite temperature correlation-driven Mott transition, the BSE diverges. The eigenvector corresponding to the divergence relates the insulating and metallic solutions that exist below the critical temperature. Particle-hole symmetry then implies that this eigenvector is antisymmetric and does not contribute to the compressibility [57], which remains finite.

The authors thank M. Capone, P. Chalupa, H. Hafermann, M. Katsnelson, A. Lichtenstein, M. Schüler, A. Toschi, A. Valli, and T. Wehling for stimulating discussions. E. G. C. P. v. L. is supported by the Zentrale Forschungsförderung of the Universität Bremen. F. K. acknowledges financial support from the Slovenian Research Agency under Project No. N1-0088. A. K. acknowledges partial financial support within the state assignment of Ministry of Science and Higher Education of the Russian Federation (theme Quant No. AAAA-A18-118020190095-4) and RFBR Grant No. 20-02-00252.

*evloon@itp.uni-bremen.de

[1] M. Imada, A. Fujimori, and Y. Tokura, Metal-insulator transitions, Rev. Mod. Phys. **70**, 1039 (1998).
[2] J. Hubbard, Electron correlations in narrow energy bands, Proc. R. Soc. A. **276**, 238 (1963).
[3] J. Kanamori, Electron correlation and ferromagnetism of transition metals, Prog. Theor. Phys. **30**, 275 (1963).
[4] M. C. Gutzwiller, Effect of Correlation on the Ferromagnetism of Transition Metals, Phys. Rev. Lett. **10**, 159 (1963).
[5] J. Hubbard, Electron correlations in narrow energy bands. III. An improved solution, Proc. R. Soc. A. **281**, 401 (1964).
[6] R. Jördens, N. Strohmaier, K. Günter, H. Moritz, and T. Esslinger, A Mott insulator of fermionic atoms in an optical lattice, Nature (London) **455**, 204 (2008).
[7] U. Schneider, L. Hackermüller, S. Will, T. Best, I. Bloch, T. A. Costi, R. W. Helmes, D. Rasch, and A. Rosch, Metallic and insulating phases of repulsively interacting fermions in a 3D optical lattice, Science **322**, 1520 (2008).
[8] R. Jördens, L. Tarruell, D. Greif, T. Uehlinger, N. Strohmaier, H. Moritz, T. Esslinger, L. De Leo, C. Kollath, A. Georges, V. Scarola, L. Pollet, E. Burovski, E. Kozik, and M. Troyer, Quantitative Determination of Temperature in the Approach to Magnetic Order of Ultracold Fermions in an Optical Lattice, Phys. Rev. Lett. **104**, 180401 (2010).
[9] P. M. Duarte, R. A. Hart, T.-L. Yang, X. Liu, T. Paiva, E. Khatami, R. T. Scalettar, N. Trivedi, and R. G. Hulet, Compressibility of a Fermionic Mott Insulator of Ultracold Atoms, Phys. Rev. Lett. **114**, 070403 (2015).
[10] D. Greif, M. F. Parsons, A. Mazurenko, C. S. Chiu, S. Blatt, F. Huber, G. Ji, and M. Greiner, Site-resolved imaging of a fermionic Mott insulator, Science **351**, 953 (2016).
[11] W. Metzner and D. Vollhardt, Correlated Lattice Fermions in $d = \infty$ Dimensions, Phys. Rev. Lett. **62**, 324 (1989).
[12] A. Georges, G. Kotliar, W. Krauth, and M. J. Rozenberg, Dynamical mean-field theory of strongly correlated fermion systems and the limit of infinite dimensions, Rev. Mod. Phys. **68**, 13 (1996).
[13] New perspectives still appear, such as topological views on the transition [14,15].
[14] D. E. Logan and M. R. Galpin, Mott insulators and the doping-induced Mott transition within DMFT: Exact results for the one-band Hubbard model, J. Phys. Condens. Matter **28**, 025601 (2015).
[15] S. Sen, P. J. Wong, and A. K. Mitchell, The Mott transition as a topological phase transition, Phys. Rev. B **102**, 081110 (R) (2020).
[16] M. Jarrell, Hubbard Model in Infinite Dimensions: A Quantum Monte Carlo Study, Phys. Rev. Lett. **69**, 168 (1992).

[17] A. Georges and W. Krauth, Numerical Solution of the $d = \infty$ Hubbard Model: Evidence for a Mott Transition, Phys. Rev. Lett. **69**, 1240 (1992).
[18] A. Georges and W. Krauth, Physical properties of the half-filled Hubbard model in infinite dimensions, Phys. Rev. B **48**, 7167 (1993).
[19] X. Y. Zhang, M. J. Rozenberg, and G. Kotliar, Mott Transition in the $d = \infty$ Hubbard Model at Zero Temperature, Phys. Rev. Lett. **70**, 1666 (1993).
[20] M. J. Rozenberg, G. Kotliar, and X. Y. Zhang, Mott-Hubbard transition in infinite dimensions. II, Phys. Rev. B **49**, 10181 (1994).
[21] R. M. Noack and F. Gebhard, Mott-Hubbard Transition in Infinite Dimensions, Phys. Rev. Lett. **82**, 1915 (1999).
[22] R. Bulla, Zero Temperature Metal-Insulator Transition in the Infinite-Dimensional Hubbard Model, Phys. Rev. Lett. **83**, 136 (1999).
[23] N. Blümer, Mott-Hubbard metal-insulator transition and optical conductivity in high dimensions, Ph.D. thesis, University of Augsburg, 2002.
[24] M. Eckstein, M. Kollar, M. Potthoff, and D. Vollhardt, Phase separation in the particle-hole asymmetric Hubbard model, Phys. Rev. B **75**, 125103 (2007).
[25] H. U. R. Strand, A. Sabashvili, M. Granath, B. Hellsing, and S. Östlund, Dynamical mean field theory phase-space extension and critical properties of the finite temperature Mott transition, Phys. Rev. B **83**, 205136 (2011).
[26] T. Schäfer, F. Geles, D. Rost, G. Rohringer, E. Arrigoni, K. Held, N. Blümer, M. Aichhorn, and A. Toschi, Fate of the false Mott-Hubbard transition in two dimensions, Phys. Rev. B **91**, 125109 (2015).
[27] A. Khurana, Electrical Conductivity in the Infinite-Dimensional Hubbard Model, Phys. Rev. Lett. **64**, 1990 (1990).
[28] V. Zlatic and B. Horvatic, The local approximation for correlated systems on high dimensional lattices, Solid State Commun. **75**, 263 (1990).
[29] T. Pruschke, D. L. Cox, and M. Jarrell, Hubbard model at infinite dimensions: Thermodynamic and transport properties, Phys. Rev. B **47**, 3553 (1993).
[30] M. J. Rozenberg, G. Kotliar, H. Kajueter, G. A. Thomas, D. H. Rapkine, J. M. Honig, and P. Metcalf, Optical Conductivity in Mott-Hubbard Systems, Phys. Rev. Lett. **75**, 105 (1995).
[31] S. Brener, H. Hafermann, A. N. Rubtsov, M. I. Katsnelson, and A. I. Lichtenstein, Dual fermion approach to susceptibility of correlated lattice fermions, Phys. Rev. B **77**, 195105 (2008).
[32] G. Rohringer, A. Valli, and A. Toschi, Local electronic correlation at the two-particle level, Phys. Rev. B **86**, 125114 (2012).
[33] L. Boehnke and F. Lechermann, Competing orders in $Na_xCoO_2$ from strong correlations on a two-particle level, Phys. Rev. B **85**, 115128 (2012).
[34] E. G. C. P. van Loon, H. Hafermann, A. I. Lichtenstein, A. N. Rubtsov, and M. I. Katsnelson, Plasmons in Strongly Correlated Systems: Spectral Weight Transfer and Renormalized Dispersion, Phys. Rev. Lett. **113**, 246407 (2014).
[35] D. Geffroy, J. Kaufmann, A. Hariki, P. Gunacker, A. Hausoel, and J. Kuneš, Collective Modes in Excitonic Magnets: Dynamical Mean-Field Study, Phys. Rev. Lett. **122**, 127601 (2019).
[36] H. U. R. Strand, M. Zingl, and N. Wentzell, Olivier Parcollet, and Antoine Georges, Magnetic response of $Sr_2RuO_4$: Quasi-local spin fluctuations due to Hund's coupling, Phys. Rev. B **100**, 125120 (2019).
[37] F. Krien, E. G. C. P. van Loon, M. I. Katsnelson, A. I. Lichtenstein, and M. Capone, Two-particle Fermi liquid parameters at the Mott transition: Vertex divergences, Landau parameters, and incoherent response in dynamical mean-field theory, Phys. Rev. B **99**, 245128 (2019).
[38] C. Melnick and G. Kotliar, Fermi liquid theory and divergences of the two-particle irreducible vertex in the periodic Anderson lattice, Phys. Rev. B **101**, 165105 (2020).
[39] A. N. Rubtsov, V. V. Savkin, and A. I. Lichtenstein, Continuous-time quantum Monte Carlo method for fermions, Phys. Rev. B **72**, 035122 (2005).
[40] P. Werner, A. Comanac, L. de' Medici, M. Troyer, and A. J. Millis, Continuous-Time Solver for Quantum Impurity Models, Phys. Rev. Lett. **97**, 076405 (2006).
[41] E. Gull, A. J. Millis, A. I. Lichtenstein, A. N. Rubtsov, M. Troyer, and P. Werner, Continuous-time Monte Carlo methods for quantum impurity models, Rev. Mod. Phys. **83**, 349 (2011).
[42] T. Schäfer, G. Rohringer, O. Gunnarsson, S. Ciuchi, G. Sangiovanni, and A. Toschi, Divergent Precursors of the Mott-Hubbard Transition at the Two-Particle Level, Phys. Rev. Lett. **110**, 246405 (2013).
[43] E. Kozik, M. Ferrero, and A. Georges, Nonexistence of the Luttinger-Ward Functional and Misleading Convergence of Skeleton Diagrammatic Series for Hubbard-Like Models, Phys. Rev. Lett. **114**, 156402 (2015).
[44] T. Schäfer, S. Ciuchi, M. Wallerberger, P. Thunström, O. Gunnarsson, G. Sangiovanni, G. Rohringer, and A. Toschi, Nonperturbative landscape of the Mott-Hubbard transition: Multiple divergence lines around the critical endpoint, Phys. Rev. B **94**, 235108 (2016).
[45] O. Gunnarsson, G. Rohringer, T. Schäfer, G. Sangiovanni, and A. Toschi, Breakdown of Traditional Many-Body Theories for Correlated Electrons, Phys. Rev. Lett. **119**, 056402 (2017).
[46] P. Chalupa, T. Schäfer, M. Reitner, D. Springer, S. Andergassen, and A. Toschi, Fingerprints of the local moment formation and its Kondo screening in the generalized susceptibilities of many-electron problems, arXiv:2003.07829.
[47] A. Stan, P. Romaniello, S. Rigamonti, L. Reining, and J. A. Berger, Unphysical and physical solutions in many-body theories: From weak to strong correlation, New J. Phys. **17**, 093045 (2015).
[48] R. Rossi and F. Werner, Skeleton series and multivaluedness of the self-energy functional in zero space-time dimensions, J. Phys. A **48**, 485202 (2015).
[49] P. Thunström, O. Gunnarsson, S. Ciuchi, and G. Rohringer, Analytical investigation of singularities in two-particle irreducible vertex functions of the Hubbard atom, Phys. Rev. B **98**, 235107 (2018).
[50] J. Vučičević, N. Wentzell, M. Ferrero, and O. Parcollet, Practical consequences of the Luttinger-Ward functional

multivaluedness for cluster DMFT methods, Phys. Rev. B **97**, 125141 (2018).
[51] W. Tarantino, P. Romaniello, J. A. Berger, and L. Reining, Self-consistent Dyson equation and self-energy functionals: An analysis and illustration on the example of the Hubbard atom, Phys. Rev. B **96**, 045124 (2017).
[52] P. Chalupa, P. Gunacker, T. Schäfer, K. Held, and A. Toschi, Divergences of the irreducible vertex functions in correlated metallic systems: Insights from the Anderson impurity model, Phys. Rev. B **97**, 245136 (2018).
[53] D. Springer, P. Chalupa, S. Ciuchi, G. Sangiovanni, and A. Toschi, Interplay between local response and vertex divergences in many-fermion systems with on-site attraction, Phys. Rev. B **101**, 155148 (2020).
[54] R. Chitra and G. Kotliar, Effective-action approach to strongly correlated fermion systems, Phys. Rev. B **63**, 115110 (2001).
[55] M. Potthoff, Self-energy-functional approach to systems of correlated electrons, Eur. Phys. J. B **32**, 429 (2003).
[56] R. Žitko, Convergence acceleration and stabilization of dynamical mean-field theory calculations, Phys. Rev. B **80**, 125125 (2009).
[57] M. Reitner, P. Chalupa, L. Del Re, D. Springer, S. Ciuchi, G. Sangiovanni, and A. Toschi, Attractive effect of a strong electronic repulsion–the physics of vertex divergences, arXiv:2002.12869.
[58] B. Bauer *et al.*, The ALPS project release 2.0: Open source software for strongly correlated systems, J. Stat. Mech. (2011) P05001.
[59] L. Huang, Y. Wang, Z. Y. Meng, L. Du, P. Werner, and X. Dai, iQIST: An open source continuous-time quantum Monte Carlo impurity solver toolkit, Comput. Phys. Commun. **195**, 140 (2015).
[60] L. Huang, iQIST v0.7: An open source continuous-time quantum Monte Carlo impurity solver toolkit, Comput. Phys. Commun. **221**, 423 (2017).
[61] H. Hafermann, P. Werner, and E. Gull, Efficient implementation of the continuous-time hybridization expansion quantum impurity solver, Comput. Phys. Commun. **184**, 1280 (2013).
[62] H. Hafermann, K. R. Patton, and P. Werner, Improved estimators for the self-energy and vertex function in hybridization-expansion continuous-time quantum Monte Carlo simulations, Phys. Rev. B **85**, 205106 (2012).
[63] Here we ignore the possibility of mixing of previous and current iterative solutions, since we are interested in the fundamental aspects of the stability of DMFT solutions.
[64] See Supplemental Material at http://link.aps.org/supplemental/10.1103/PhysRevLett.125.136402 for detailed derivations of the impurity and Landau thermodynamic potentials, the Jacobian for DMFT self-consistency, and the relation between different functionals.
[65] A. N. Rubtsov, M. I. Katsnelson, and A. I. Lichtenstein, Dual fermion approach to nonlocal correlations in the Hubbard model, Phys. Rev. B **77**, 033101 (2008).
[66] H. Hafermann, Numerical approaches to spatial correlations in strongly interacting fermion systems, Ph.D. Thesis, University of Hamburg, 2010.
[67] G. Rohringer, H. Hafermann, A. Toschi, A. A. Katanin, A. E. Antipov, M. I. Katsnelson, A. I. Lichtenstein, A. N. Rubtsov, and K. Held, Diagrammatic routes to nonlocal correlations beyond dynamical mean field theory, Rev. Mod. Phys. **90**, 025003 (2018).
[68] E. G. C. P. van Loon, H. Hafermann, A. I. Lichtenstein, and M. I. Katsnelson, Thermodynamic consistency of the charge response in dynamical mean-field based approaches, Phys. Rev. B **92**, 085106 (2015).
[69] G. Kotliar, Landau theory of the Mott transition in the fully frustrated Hubbard model in infinite dimensions, Eur. Phys. J. B **11**, 27 (1999).
[70] G. Kotliar, E. Lange, and M. J. Rozenberg, Landau Theory of the Finite Temperature Mott Transition, Phys. Rev. Lett. **84**, 5180 (2000).
[71] G. V. Astretsov, G. Rohringer, and A. N. Rubtsov, Dual parquet scheme for the two-dimensional Hubbard model: Modeling low-energy physics of high-$T_c$ cuprates with high momentum resolution, Phys. Rev. B **101**, 075109 (2020).
[72] G. Kotliar, S. Murthy, and M. J. Rozenberg, Compressibility Divergence and the Finite Temperature Mott Transition, Phys. Rev. Lett. **89**, 046401 (2002).
[73] H. Hafermann, E. G. C. P. van Loon, M. I. Katsnelson, A. I. Lichtenstein, and O. Parcollet, Collective charge excitations of strongly correlated electrons, vertex corrections, and gauge invariance, Phys. Rev. B **90**, 235105 (2014).
[74] P. Werner, E. Gull, M. Troyer, and A. J. Millis, Spin Freezing Transition and Non-Fermi-Liquid Self-Energy in a Three-Orbital Model, Phys. Rev. Lett. **101**, 166405 (2008).
[75] K. Haule and G. Kotliar, Coherence–incoherence crossover in the normal state of iron oxypnictides and importance of Hund's rule coupling, New J. Phys. **11**, 025021 (2009).
[76] L. de' Medici, S. R. Hassan, M. Capone, and X. Dai, Orbital-Selective Mott Transition out of Band Degeneracy Lifting, Phys. Rev. Lett. **102**, 126401 (2009).
[77] L. de' Medici, J. Mravlje, and A. Georges, Janus-Faced Influence of Hund's Rule Coupling in Strongly Correlated Materials, Phys. Rev. Lett. **107**, 256401 (2011).
[78] P. Werner, M. Casula, T. Miyake, F. Aryasetiawan, A. J. Millis, and S. Biermann, Satellites and large doping and temperature dependence of electronic properties in hole-doped $BaFe_2As_2$, Nat. Phys. **8**, 331 (2012).
[79] K. M. Stadler, Z. P. Yin, J. von Delft, G. Kotliar, and A. Weichselbaum, Dynamical Mean-Field Theory Plus Numerical Renormalization-Group Study of Spin-Orbital Separation in a Three-Band Hund Metal, Phys. Rev. Lett. **115**, 136401 (2015).
[80] L. de' Medici, Hund's Induced Fermi-Liquid Instabilities and Enhanced Quasiparticle Interactions, Phys. Rev. Lett. **118**, 167003 (2017).
[81] P. V. Arribi and L. de' Medici, Hund-Enhanced Electronic Compressibility in FeSe and Its Correlation with $T_c$, Phys. Rev. Lett. **121**, 197001 (2018).
[82] M. Grilli, R. Raimondi, C. Castellani, C. Di Castro, and G. Kotliar, Superconductivity, Phase Separation, and Charge-Transfer Instability in the $U = \infty$ Limit of the Three-Band Model of the $CuO_2$ Planes, Phys. Rev. Lett. **67**, 259 (1991).
[83] P. Majumdar and H. R. Krishnamurthy, Lattice Contraction Driven Insulator-Metal Transition in the $d = \infty$ Local Approximation, Phys. Rev. Lett. **73**, 1525 (1994).

[84] A. Tandon, Z. Wang, and G. Kotliar, Compressibility of the Two-Dimensional Infinite-$U$ Hubbard Model, Phys. Rev. Lett. **83**, 2046 (1999).

[85] K. Held, A. K. McMahan, and R. T. Scalettar, Cerium Volume Collapse: Results from the Merger of Dynamical Mean-Field Theory and Local Density Approximation, Phys. Rev. Lett. **87**, 276404 (2001).

[86] M. Capone, G. Sangiovanni, C. Castellani, C. Di Castro, and M. Grilli, Phase Separation Close to the Density-Driven Mott Transition in the Hubbard-Holstein Model, Phys. Rev. Lett. **92**, 106401 (2004).

[87] M. Aichhorn, E. Arrigoni, M. Potthoff, and W. Hanke, Phase separation and competition of superconductivity and magnetism in the two-dimensional Hubbard model: From strong to weak coupling, Phys. Rev. B **76**, 224509 (2007).

[88] S. Lupi, L. Baldassarre, B. Mansart, A. Perucchi, A. Barinov, P. Dudin, E. Papalazarou, F. Rodolakis, J.-P. Rueff, J.-P. Itié *et al.*, A microscopic view on the Mott transition in chromium-doped $V_2O_3$, Nat. Commun. **1**, 105 (2010).

[89] J. Otsuki, H. Hafermann, and A. I. Lichtenstein, Superconductivity, antiferromagnetism, and phase separation in the two-dimensional Hubbard model: A dual-fermion approach, Phys. Rev. B **90**, 235132 (2014).

[90] C.-H. Yee and L. Balents, Phase Separation in Doped Mott Insulators, Phys. Rev. X **5**, 021007 (2015).